



1 **Mangrove sediment organic carbon storage and sources in relation to forest age**
2 **and position along a deltaic salinity gradient**

3

4 Rey Harvey Suello¹, Simon Lucas Hernandez^{1,5}, Steven Bouillon², Jean-Philippe Belliard¹, Luis
5 Dominguez-Granda³, Marijn Van de Broek⁴, Andrea Mishell Rosado Moncayo³, John Ramos Veliz³,
6 Karem Pollette Ramirez³, Gerard Govers², Stijn Temmerman¹

7

8 ¹ University of Antwerp, Ecosystem Management Research Group, ² Katholieke Universiteit Leuven, Divi-
9 sion of Soil and Water Management, ³ Escuela Superior Politecnica del Litoral, Department of Sustainable
10 Water Management, ⁴ Swiss Federal Institute of Technology, Department of Environmental Systems Science,
11 ⁵ Ghent University, Laboratory of Environmental Toxicology and Aquatic Ecology

12

13 Correspondence to: Rey Harvey Suello, Ecosystem Management Research Group (ECOBE), University of
14 Antwerp, Antwerp, Belgium (suello.reyharvey@uantwerpen.be)

15

16 **Abstract**

17

18 Mangroves are widely recognised as key ecosystems for climate change mitigation as they capture and
19 store significant amounts of sediment organic carbon (SOC). Yet, there is incomplete knowledge on
20 how sources of SOC and their differential preservation vary between mangrove sites in relation to envi-
21 ronmental gradients. To address this, sediment depth profiles were sampled from mangrove sites ranging
22 from river-dominated to marine-dominated sites and including old and young mangrove sites, in the
23 Guayas delta (Ecuador). The stable carbon isotope ratios ($\delta^{13}\text{C}$) and the elemental composition (OC%,
24 C:N) of sediment profiles, local vegetation (i.e., autochthonous carbon) and externally-supplied sus-
25 pended particulate matter (i.e., allochthonous carbon) were obtained to assess variations in the amount
26 and sources of SOC at different locations throughout the delta. In general, across all sites, we found
27 increasing SOC contents and stocks are associated with decreasing $\delta^{13}\text{C}$ and increasing C/N ratios, indicating



28 that SOC stocks and sources are intrinsically related. The SOC stocks (down to 0.64 m deep profiles) are
29 significantly lower in young mangrove sites (46-55 Mg C ha⁻¹) than in old sites (78 - 92 Mg C ha⁻¹). The
30 SOC in the young mangrove sites is mainly of allochthonous origin (estimated on average at 79%)
31 whereas in the old sites there is a slight dominance of autochthonous OC (on average 59%). Moreover,
32 from river- to marine-dominated sites, a pattern was found of increasing SOC stocks and increasing
33 autochthonous SOC contribution. These observed differences along the two studied gradients are hy-
34 pothesized to be mainly driven by (1) expected higher sedimentation rates in the river-dominated and
35 lower-elevation younger sites, thereby ‘diluting’ the SOC content and decreasing the relative autoch-
36 thonous contribution; and (2) potential differences in preservation of the different SOC sources. Our
37 finding of high contributions of allochthonous SOC, especially in young mangroves, implies that this
38 carbon is not originating from CO₂ sequestration by the mangrove ecosystem itself, but is externally
39 supplied from other terrestrial, marine or estuarine ecosystems. We argue that accounting for lower SOC
40 stocks and higher contribution of allochthonous SOC in young and river-dominated mangrove sites, as
41 compared to old and marine-dominant sites, is particularly relevant for designing and valuing nature-
42 based climate mitigation programs based on mangrove reforestation.

43

44 KEYWORDS

45 blue carbon, sediment organic carbon, stable carbon isotope, autochthonous, allochthonous, climate change,
46 Guayas delta

47

48

49

50

51

52

53

54

55

56



57 1 | INTRODUCTION

58

59 Situated at the interface between terrestrial and marine environments, mangrove forests are unique wetland
60 ecosystems occupying (sub-)tropical intertidal zones (Burkett & Kusler, 2000; Duke et al., 2007; Polidoro et
61 al., 2010; Tue et al., 2012). They provide a myriad of ecosystem services, such as their ability to contribute
62 to global climate regulation by effectively sequestering carbon (Donato et al., 2011; Mcleod et al., 2011;
63 Taillardat et. al., 2018). Mangroves accumulate carbon at an estimated rate of 20-949 g C m⁻² yr⁻¹, accounting
64 for more than 10% of the carbon sequestration by the global ocean (Mcleod et al., 2011; Alongi, 2014), while
65 mangroves only cover ca. 2 % of the global ocean (Duarte et al., 2004). Compared to other ecosystem types,
66 such as rain forests, peat swamps, salt marshes and seagrasses, mangroves store much higher carbon stocks
67 which approximately range from 140 - 1023 Mg C ha⁻¹ (Donato et al., 2011; Alongi, 2014; Schile et al.,
68 2017). This demonstrates the importance of the carbon capture and storage capacity of mangrove ecosystems.
69 Recent estimations by Atwood et al. (2017) equate to 2.6 billion Mg of C stored in mangrove sediments down
70 to a 1 m depth worldwide.

71

72 This high capacity of mangroves to store carbon is to a large extent due to the accumulation of organic
73 carbon into their sediments through a range of mechanisms. Generally, sediment organic carbon (SOC) orig-
74 inates from autochthonous inputs (i.e. from local biomass production) and allochthonous inputs (i.e. from
75 particulate sediment deposition during tidal inundation) that are well-preserved by the mostly anoxic sedi-
76 ment conditions in mangroves (Kristensen, 2008). Above and belowground biomass accumulates in man-
77 grove sediments through litterfall, vegetation die-off, root exudation and root growth, and this constitutes the
78 autochthonous SOC in mangrove sediments. On the other hand, during regular tidal flooding events man-
79 groves trap allochthonous carbon from tidal waters containing fine sediment particles from marine, estuarine,
80 and terrestrial origin (Alongi, 2014). These organic materials of both autochthonous and allochthonous origin
81 are stored and buried in the mangrove sediments, through sedimentation (during high tides and high-energy
82 events like storm surges) and bioturbation (e.g. burrowing of crustaceans). The preservation of this buried
83 SOC is dependent on, among other factors, organic matter sorption to mineral substrates, microbial decom-
84 position activity (Kristensen et al., 2008; Adame et al., 2015) and tide-driven groundwater fluxes (Maher et
85 al., 2013).



86 Unveiling environmental gradients that affect variations in the amount of allochthonous and autochtho-
87 nous SOC in mangroves is highly relevant, since the fate and long-term preservation of these two SOC
88 sources may differ. Recent field studies in temperate-climate tidal marshes indicate that locally produced
89 autochthonous SOC is abundantly present in the top 5-20 cm of sediment profiles, but is largely lost with
90 increasing depth beneath the sediment surface, due to mineralization and leaching. In contrast, long-term
91 preserved SOC is to a large extent of external allochthonous origin, suggesting this SOC source is more
92 protected against mineralization (Van de Broek et al. 2018; Mueller et al. 2019). Furthermore, discriminating
93 between autochthonous and allochthonous SOC sources is important, especially to properly assess the mag-
94 nitude to which this ecosystem can help mitigate climate change. After all, it is only the autochthonous SOC
95 that is assimilated from atmospheric CO₂ within the mangrove ecosystem itself, while the allochthonous SOC
96 originates from externally supplied organic C from other upstream (terrestrial), downstream (marine) or es-
97 tuarine ecosystems. In that respect, double accounting of allochthonous OC has to be avoided in carbon
98 budgets (Van den Broek et al. 2018) as this SOC is originally sequestered in another environment. Yet the
99 burial of allochthonous OC into mangrove SOC is relevant, as that OC may have contributed otherwise to
100 greenhouse gas emissions from estuarine waters (Barr et al., 2010; Borges & Abril, 2011; Sturm et al., 2017;
101 Jacotot et al. 2018). Thus, making a distinction between allochthonous and autochthonous SOC is crucial.
102 However, there is limited knowledge on the relative contribution of the autochthonous and allochthonous
103 inputs to SOC in mangroves and specifically how this contribution may vary spatially in relation to environ-
104 mental gradients.

105

106 The scarce number of studies on tidal marshes in temperate climate zones might provide hypotheses on
107 which environmental gradients may be relevant for tropical mangroves. Here we focus on two gradients, for
108 reasons argued below: (1) a deltaic or estuarine gradient from seaward sites (marine dominated) to landward
109 sites (riverine dominated), and (2) young and old mangroves. Available studies from tidal marshes show a
110 general pattern of decreasing SOC contents along estuarine salinity gradients from land to sea (Abril et al.,
111 2002; Craft et al., 2007; Wieski et al., 2010; Hansen et al., 2016; Van de Broek et al., 2016), and this may be
112 associated with shifts in the allochthonous versus autochthonous contributions to marsh SOC. For example,
113 in studies of tidal marshes in the US (Craft et al., 2007) and in Belgium and the Netherlands (Van de Broek



114 et al., 2016), it was found that tidal marshes located more upstream along estuaries predominantly store SOC
115 from allochthonous riverine inputs, due to higher contents of suspended particulate matter (SPM) and partic-
116 ulate organic carbon (POC), hence leading to higher rates of allochthonous SOC accumulation and higher
117 SOC stocks in more upstream marsh sites. Further, young low-elevation marshes that established more re-
118 cently on mudflats, are often characterized by higher rates of allochthonous sediment deposition, as compared
119 to higher-elevation older marsh sites (Temmerman et al., 2004; Kirwan et al., 2016), and therefore it may be
120 hypothesized that the SOC in young sites contains more allochthonous carbon as compared to old sites.
121 However, it still remains to be investigated if such patterns on allochthonous versus autochthonous SOC
122 sources and preservation, in relation to wetland age and position along an estuarine land-to-sea gradient, as
123 found for temperate zone tidal marshes (Van de Broek et al., 2016; Van de Broek et al., 2018, Mueller et al.,
124 2019), also occur in tropical mangroves, which obviously differ from marshes in many respects such as veg-
125 etation type, canopy density, and climate, among others.

126

127 While it is widely accepted that mangroves act as major carbon sinks (Bouillon et al., 2008; Nelleman
128 et al., 2008, Atwood et al., 2017; Marchand et al., 2017; Jennerjahn, 2020), at present, there are no studies
129 that specifically investigated the stocks and sources of SOC in relation to the age and position of mangroves
130 along the land-to-sea gradient within a delta or estuary. Therefore, this study aims at quantifying and identi-
131 fying first-order controls of SOC stocks and sources (allochthonous versus autochthonous) along an estuarine
132 land-to-sea gradient and between old and young mangrove forest sites in the Guayas Delta, Ecuador.

133

134 **2 | MATERIALS AND METHODS**

135

136 **2.1 | Study site**

137

138 Field sampling was conducted in the Guayas Delta (Ecuador) which borders the Gulf of Guayaquil (Figure
139 1), together forming the largest estuarine system along the Pacific coast of South America (Cucalon, 1989;
140 Reynaud et al., 2018). Its geomorphology consists of multiple branching river channels that intersect a large
141 deltaic plain with approximately 4000 km² of mangroves (Reynaud et al., 2018). Tidal gauge stations within
142 the delta operated by Instituto Oceanográfico de la Armada del Ecuador (INOCAR, Oceanographic Institute



143 of the Navy, Figure 1) recorded mean long-term (1984 -2016) tidal ranges of 2.12, 2.85, and 3.42 m and sea
144 level rise rates of 1.7, 4.9, and 4.0 mm/yr for stations Puerto Bolivar, Puná and Rio Guayas, respectively.

145

146 Two main estuarine sub-systems can be distinguished within the delta. To the east is the Guayas River
147 estuary, which is a river-influenced estuary exhibiting a salinity gradient that ranges from 0-2 at the landward
148 side of the tidal influence to 30 ppt at the delta mouth during the yearly dry season (June to November),
149 dropping down at the latter location to 15-20 during the wet season (December to May) (Arreaga Vargas,
150 2000). To the west is the Estero El Salado estuary, which is a former tributary of the Guayas River that is
151 now disconnected from freshwater river discharge at its northern limit, making it a marine-dominated estua-
152 rine system with salinity levels higher than in the Guayas River, ranging from 23.4 – 32.7 (Cifuentes et al.,
153 1996; Twilley et al., 1998; Reynaud et al., 2018). Rainfall in the Guayas River catchment is seasonal, with
154 95 % of precipitation occurring in the rainy season. As a result, the Guayas River has an average monthly
155 discharge of 1400 m³/s, ranging from 200 m³/s in the dry season to 1600 m³/s in the rainy season, during a
156 year of average precipitation (Cifuentes et al. 1996; Twilley et al., 2001).

157

158 Eight sampling locations (see Table S1 for coordinates) were identified in these two subsystems, consist-
159 ing of four paired sets of young and old mangrove sites that are located nearby each other (Figure 1). These
160 four pairs of young/old sites were situated in four sampling zones with different position in the delta. Three
161 different sampling zones were selected along the Guayas River estuary. These three sampling zones are re-
162 ferred to as the Upstream, Intermediate and Downstream zones (Figure 1). A fourth sampling zone was se-
163 lected in the marine-dominated El Salado estuary, which is further referred to as the Marine zone. Based on
164 an analysis of historical LANDSAT satellite images, we selected within each zone a young mangrove site
165 (only emerging on satellite images at least after 1993 by mangrove establishment on initially bare mudflats)
166 and an old mangrove site (visible as established mangroves on satellite images older than 1984). There is a
167 strong dominance of *Rhizophora somoensis* in the old sites and *Avicennia germinans* in the young sites of
168 the intermediate, downstream and marine zones, whereas the young and old sites of the upstream zone show
169 high diversity of mangroves (*Rhizophora* and *Avicennia*) and an understory of freshwater plant species. Trees



170 on the old sites have stem diameters mostly between 0.5 and 1 m, while on young sites this was mostly
171 between 0.1 and 0.5 m, confirming we had selected contrasting old and young sites.

172

173 **2.2 | Sample collection**

174

175 Sediment cores were collected in September 2018 using cylindrical PVC tubes (0.10 m diameter), inserted
176 manually down to a minimum depth of 0.64 m. At each site, 3 replicate sediment cores were sampled with
177 an approximate maximum distance of 3 meters per coring location, resulting in a total of 24 sediment cores.

178 Aboveground biomass samples (sun-shaded and sun-exposed green leaves, senescent leaves, leaf litter, live
179 twigs and branches) were collected in the field on all sampling locations, as well as belowground biomass
180 (light-colored roots) were manually sampled from the sediment cores in the lab, to represent autochthonous
181 mangrove biomass. Surface water samples for determination of allochthonous suspended particulate organic
182 carbon (POC) concentration were also collected from the river channels directly adjacent to each mangrove
183 site with a 3 L Niskin bottle from just below the water surface and stored in 1 L opaque plastic bottles in a
184 cool box filled with ice. Water samples were taken during a high water and low water campaign, both during
185 the dry season (September 2018) and wet season (March 2019).

186

187 All samples (sediment and biomass) were transported and immediately frozen at the laboratory. The fro-
188 zen sediment cores were mechanically sliced per centimeter, thawed and then oven-dried at 60°C for 48
189 hours. Biomass samples were oven-dried using the same procedure. Total suspended matter (TSM) and POC
190 content of the TSM were determined by filtering a known volume of water through pre-weighed and pre-
191 combusted 47 mm and 25 mm Whatmann GF/F filters (nominal pore size 0.7 µm), respectively.

192

193 **2.3 | Sample analyses**

194

195 From each core, subsamples (i.e., slices of 0.01 m depth increments) were taken every 0.04 m. To obtain the
196 sediment bulk density the samples were oven-dried at 60°C for 48 hours and were desiccated for 30-minutes
197 to constant weight. Large pieces of living macroscopic vegetation residues (i.e., light colored roots) were



198 then manually removed and kept as belowground biomass samples, while the remaining sediment samples
199 were homogenized. All samples were treated with 10% HCl solution after weighing them into silver cups to
200 remove carbonates, and were left overnight in an oven at 50°C. These were then analyzed for OC content,
201 C:N ratios and $\delta^{13}\text{C}$ using an Elemental Analyzer (Thermo EA 1110 coupled to a Thermo Delta V Advantage
202 isotope ratio mass spectrometer). For the analysis of grain size distribution, subsamples were taken every
203 0.08 m for each core and were analyzed using a LS 13 320 Laser Diffraction Particle Size Analyzer. The
204 grain size was classified to fractions of clay (<2 μm), silt (<2-63 μm) and sand (>63 μm).

205

206 Before analysis of the plant materials, the samples were pulverized using a mortar and pestle. The re-
207 maining samples with harder composition were powdered using a mechanical ball mill or after treatment
208 with liquid nitrogen. The ground samples were then weighed into tin cups. The filters used to collect POC in
209 TSM samples, on the other hand were exposed to HCl fumes for 4 hours to remove inorganic carbon and
210 dried at 50 °C overnight. Hereafter, filters were encapsulated in silver cups and stored in well plates. All plant
211 materials and filters were analyzed for OC, C:N and $\delta^{13}\text{C}$ using the same EA-IRMS setup as for the sediment
212 core samples.

213

214

215 **2.4 | Data analysis**

216 **2.4.1 | OC Stocks Calculation**

217

218 For the analysis of depth profiles of OC%, $\delta^{13}\text{C}$ and C:N ratios, all replicate cores were analyzed at 0.04 m
219 depth intervals. As the replicate cores have varying sampling depths, depth profiles were analyzed up to a
220 maximum common depth of 0.64 m for the three replicates per location. For the determination of OC stocks,
221 continuous depth profiles of SOC content and bulk density were first obtained by linear interpolation. The
222 OC density (g cm^{-3}) was then obtained by multiplying the interpolated OC (%) and bulk density (g cm^{-3})
223 values. The total OC stocks (Mg OC ha^{-1}) from each site were finally determined by summing up OC density
224 at all depth intervals and then multiplying the values by the depth interval (cm). Compaction during sample
225 collection was taken into account in the calculation of OC stocks.



226 2.4.2 | Two End-Member Mixing Model

227

228 To identify the sources and examine the factors controlling the accumulation of organic carbon in mangrove
229 sediments, two end-member mixing curves were made describing the relationship between OC% and $\delta^{13}\text{C}$
230 values, and between C/N and $\delta^{13}\text{C}$ values. Organic carbon derived from local (autochthonous) and external
231 (allochthonous) inputs are expected to exhibit different $\delta^{13}\text{C}$ values. With this, two end-members, namely the
232 $\delta^{13}\text{C}$ ratio of the POC of the estuarine waters (allochthonous component) and of the above and belowground
233 vegetation biomass (autochthonous component), were considered. The input parameter values were calcu-
234 lated using averages of the POC and vegetation data. The definition of these components was necessary to
235 calculate the expected $\delta^{13}\text{C}$ values of sediments for a given C/N or OC%. The latter calculation was done
236 using the equations derived by Bouillon *et al.*, (2003). First, the fraction of the bulk sediment which is from
237 mangrove origin, X_{mangrove} , was calculated as:

238

$$239 \quad X_{\text{mangrove}} = \frac{C_{\text{sediment}} (\%) - C_{\text{allocht}} (\%)}{C_{\text{mangrove}} (\%) - C_{\text{allocht}} (\%)} \quad (1)$$

240

$$0 < X_{\text{mangrove}} < 1 \quad (1)$$

241

242 Where C_{sediment} , C_{allocht} , and C_{mangrove} corresponds to the OC content (%) of the sediment, of the alloch-
243 thonous particulate organic carbon and of the autochthonous vegetation, respectively. The result obtained
244 from the equation above was correspondingly used to calculate the fraction of OC in the sediment that is of
245 autochthonous mangrove origin, $X_{\text{mangroveC}}$ (%), as:

246

$$247 \quad X_{\text{mangroveC}} = \frac{X_{\text{mangrove}} - C_{\text{mangrove}} (\%)}{X_{\text{mangrove}} * C_{\text{mangrove}} (\%) + (1 - X_{\text{mangrove}}) * C_{\text{allocht}} (\%)} \quad (2)$$

248

$$0 < X_{\text{mangroveC}} < 1$$

249

250 Finally, the expected $\delta^{13}\text{C}$ of the sediment organic matter, $\delta^{13}\text{C}_{\text{sediment}} (\text{‰})$, was calculated as:



251

$$252 \quad \delta^{13}C_{\text{sediment}} (\text{‰}) = X_{\text{mangroveC}} * \delta^{13}C_{\text{mangrove}} (\text{‰}) + (1 - X_{\text{mangroveC}}) * \delta^{13}C_{\text{allocht}} (\text{‰}) \quad (3)$$

253

254 Where $\delta^{13}C_{\text{mangrove}} (\text{‰})$ and $\delta^{13}C_{\text{allocht}} (\text{‰})$ correspond to the stable carbon isotopic composition of the
255 autochthonous mangrove vegetation and allochthonous estuarine POC, respectively. For the relationship be-
256 tween the sediment $\delta^{13}C$ values and C:N ratios, similar equations were derived.

257

258 **2.4.3 | Statistical Analyses**

259

260 To test whether the OC%, $\delta^{13}C$ and C:N significantly differed between the young and old sites, paired t-tests
261 were performed. One-way Analysis of Variance (ANOVA) was used to test if the same parameters and the
262 OC stocks were statistically significantly different between zones (upstream, intermediate, downstream, and
263 marine). All data were checked for normality (Shapiro-Wilk) and homogeneity of variances (Levene's Test)
264 with a level of significance of $p < 0.05$. Appropriate transformations (log & box cox) were performed for data
265 that were not normally distributed and corresponding non-parametric tests (Mann-Whitney & Kruskal-Wal-
266 lis) were employed for data that remained non normal after transformations. The data were analyzed using R
267 programming (R Core Team, 2017).

268

269 **3 | RESULTS**

270 **3.1 | Sediment organic carbon (SOC) depth profiles**

271 The SOC contents of the sampled mangrove sediments varied considerably from 1.10 to 7.80% (Figure 2).
272 The SOC contents of the old mangrove sites were significantly higher than for the young counterparts (Up-
273 stream: T-test, $T(5)=4.76$; $p < 0.005$; Intermediate: T-test, $T(5)=11.68$; $p < 0.05$; Downstream: T-test,
274 $T(5)=12.01$; $p < 0.005$) (Fig. 2 and Table S2). On the other hand, the SOC contents of the young and old sites
275 in the Marine zone were not significantly different (T-test, $T(5)=2.59$; $p > 0.05$). A general pattern of increas-
276 ing SOC content was observed from Upstream to Downstream sites and the values were found to significantly
277 differ between these sites (Kruskall-Wallis, Chi-Square=68.29; $p < 0.001$) (Fig. 2 and Table S2). The SOC



278 content for each site showed a relatively uniform distribution over depth (Figure 2), with some minor varia-
279 tions with depth for certain sites (Intermediate Old, Downstream Old and Marine sites).

280 **3.2 | Inventories of sediment organic carbon stocks**

281 A direct comparison between sites was done after calculating the SOC stocks down to the maximum common
282 depth of 0.64 m, showing SOC stocks varying between 46.6 ± 0.3 and 98.3 ± 1.9 Mg C ha⁻¹ (Figure 3 and
283 Table S3 and Figure S1). First, the SOC stocks were significantly higher on old sites as compared to young
284 sites (T-test, T(5)=2.80; p<0.005). Secondly, the SOC stocks were found to significantly increase (ANOVA,
285 F_{6,14}= 12.39; P<0.001) from upstream to downstream, at least for the old sites (Figure 3 and Table S2). The
286 young and old sites of the Marine zone had SOC stocks (97.74 ± 1.52 and 92.7 ± 0.93 Mg C ha⁻¹, respectively)
287 that are comparable to the Intermediate and Downstream old mangrove sites.

288

289 **3.4 | Stable carbon isotope ratios in sediments and potential sources**

290 Figure 4A-D shows the $\delta^{13}\text{C}$ values of SOC along the sediment depth profiles, together with the $\delta^{13}\text{C}$ values
291 of the above and belowground vegetation and POC of the adjacent water bodies. The sediment $\delta^{13}\text{C}$ values
292 of the sediment cores are 6-10‰ higher relative to the average vegetation of the sites (Table S2 and S4) and
293 varied between -28.1 and -24.4‰. In contrast, the average $\delta^{13}\text{C}$ values of the POC of the adjacent water
294 bodies (circles) in the Upstream, Intermediate and Downstream sites were found to correspond closer to the
295 sediment $\delta^{13}\text{C}$ values, with the $\delta^{13}\text{C}$ value of sedimentary OC being lower compared to values for riverine
296 POC (Table S5). Furthermore, $\delta^{13}\text{C}$ values of the older sites (at the Intermediate, Downstream and Marine
297 sites) are more negative than the younger sites (Fig. 4; Table S2 and Figure S2). Comparison between the
298 young and old sites revealed that these differences were statistically significant at the Upstream, Intermediate
299 and Downstream zones (T-test, T₅=2.78, T₅=41.25, and T₅=89.48; p<0.005, respectively). A generally ho-
300 mogeneous pattern of $\delta^{13}\text{C}$ values with depth was observed in all the sites, except the Upstream old site (Fig.
301 4A-D).

302

303

304 **3.5 | Two end-member mixing model**



305 The $\delta^{13}\text{C}$ was plotted against the elemental ratios (C/N) and SOC content (%) of the sediments from all sites
306 (Figures 5A and 5B). Figure 5A showed a negative correlation ($r = -0.76$) between the $\delta^{13}\text{C}$ values and the
307 SOC content of the sediment samples. An inverse relationship ($r = -0.69$) was also observed between C/N
308 ratios and $\delta^{13}\text{C}$ values (Figure 5B.). The SOC content and C/N of the POC from the suspended particulate
309 matter of the adjacent estuarine waters were particularly low (1.45– 3.24% and 7.3 – 9.5, respectively) and
310 corresponded to less negative $\delta^{13}\text{C}$ values (-25.1 to -27.2‰). On the other hand, the SOC content and C/N of
311 the vegetation samples were found to be higher (26.5 -47.6 % and 27.1 – 47.2, respectively) and were matched
312 with lower $\delta^{13}\text{C}$ values (-33.7 to -29.0‰).

313 Mixing model curves were calculated then from the data (Fig. 5). The average mixing curves (referred to
314 as “mixing mid” in Fig. 5A and B) were obtained using the average observed POC and vegetation data as
315 input values for the model parameters in equations 1-3. To account for the uncertainty of the parameter val-
316 ues, they were also varied to obtain minimum and maximum mixing curves (“mixing min” and “mixing max”
317 in Fig. 6A and B). After checking the degree of sensitivity of the resulting mixing curves to the variations in
318 input values, a slight variation of values was applied ($\delta^{13}\text{C}_{\text{allocht}}$ between -27.0 and -25.2‰, $\delta^{13}\text{C}_{\text{mangrove}}$ be-
319 tween -33.0 and -27‰, $\text{OC}_{\text{sediment}}$ between 0.6 and 1.5%, $\text{C:N}_{\text{mangrove}}$ between 42 and 60), resulting in the
320 minimum and maximum mixing curves in Figures 5A and B. Overall the obtained mixing curves encompass
321 the observed data reasonably well.

322

323 **3.6 | Stable carbon isotope ratios in sediments and potential sources**

324 Estimations on the relative contribution (%) of allochthonous and autochthonous origin to the SOC (Figure
325 6, see Table S4 for specific values of all sites) show that overall, the sampled mangrove sediments pre-
326 dominantly contain externally supplied allochthonous carbon (estimated at 65 %) rather than locally pro-
327 duced autochthonous carbon. Younger sites also have more allochthonous carbon (79 ± 17 %) whereas
328 older sites have slightly more autochthonous carbon (59 ± 8 %) stored in the sediments. While the contribu-
329 tion of allochthonous carbon was consistently higher for all sites, a general pattern of increasing contribu-
330 tion of autochthonous carbon from the upstream to the downstream and marine zones was observed (Figure
331 6).



332

333 **4 | DISCUSSION**

334

335 Despite widespread recognition of mangroves as key ecosystems for climate change mitigation through C
336 capture and storage (Mcleod et al., 2011; Pendelton et al., 2012; Siikamäki et al., 2012; Murdiyarso *et al.*,
337 2015), relatively limited knowledge is available on the variability in amounts and sources of sediment organic
338 carbon in relation to environmental gradients within a system, such as mangrove age and position along an
339 estuarine land-to-sea gradient. Our study on the Guayas delta (Ecuador) shows that SOC stocks and contents
340 on old sites increase from river-dominated to marine-dominated sites and are generally lower in young sites
341 as compared to old sites. Across all sites, increasing SOC contents are associated with decreasing $\delta^{13}\text{C}$ and
342 increasing C/N ratios. This suggests that the sources of SOC are predominantly of allochthonous origin for
343 younger sites (on average 79%), while for older sites there is a slight dominance of autochthonous SOC origin
344 (on average 59%). In the following section we explore potential mechanisms and hypotheses that may explain
345 these observations, and we discuss implications for managing mangroves for carbon capture and storage.

346

347 **4.1 | SOC variability between young and old mangrove sites**

348

349 The majority of the old mangrove sites along the Guayas Delta had a significantly higher SOC stock and
350 content than the young sites (Figure 2 and Figure 3). As a first potential explanation, we hypothesize this is
351 due to a SOC ‘dilution effect’ that is, as explained below, related to differences in suspended sediment ac-
352 cretion rates between old and young mangrove sites. Several authors (Pethick, 1981; Allen, 1990; French,
353 1993; Temmerman et. al., 2003; Kirwan et al. 2016) have shown that more recently formed (young) tidal
354 marshes experience higher sediment accretion rates than their older counterparts. This is because new
355 (young) marsh formation, through establishment of pioneer vegetation on initially unvegetated intertidal flats,
356 starts at a lower elevation relative to mean sea level as compared to the higher elevation of established old
357 marshes. Hence younger, lower-elevation marshes are subject to a higher tidal inundation frequency, depth
358 and duration, and therefore higher rate of suspended sediment supply and deposition. Applying this analogy
359 in mangroves, it is therefore reasonable to assume that the sampled sediment profiles in our young mangrove



360 sites (formed after 1984 by mangrove establishment on originally unvegetated intertidal flats) have accreted
361 at higher rates than at the adjacent old mangrove sites (already established, based on analysis of remote
362 sensing images, at least before 1984). We expect that the higher volume of tidally supplied sediment input in
363 young sites largely consists of mineral suspended sediments that are relatively low in POC content (Duarte
364 et al. 2004; Saintilan et al. 2013; Alongi, 2014). This is confirmed by our SPM samples, which showed a low
365 POC content of 1.45 to 3.24 %. Higher suspended sediment accretion rates on young mangroves, would result
366 then in a ‘dilution effect’ of the locally produced mangrove organic matter which typically has higher OC
367 content. In line with our findings, other studies have also suggested that the organic carbon stock in mangrove
368 sediments increases linearly with the mangrove forest age as biomass-derived C significantly increased in
369 older compared to younger forests (Lovelock et al. 2010; Marchand 2017).

370

371 Additionally, the higher frequency and duration of tidal inundation in the lower-elevated young mangrove
372 sites is expected to promote more tidal currents that could cause export of POC from macroscopic origin
373 (litter of leaves, twigs, barks, ...) that could otherwise have been buried in the system. Furthermore, older
374 mangrove sites generally have a denser tree canopy and root structure than young mangrove sites, which was
375 shown by Alongi (2012) to hinder tidal export of litter from the forest sediment surface. It has also been
376 proposed that the sediments of younger mangroves, with lower surface elevations and more frequent tidal
377 inundations, are more often in less reducing conditions due to daily renewal of electron acceptors (e.g. man-
378 ganese and iron) with tides and oxygen diffusion by the *Avicennia* root systems (Marchand et al. 2004, 2006).
379 These conditions may have also contributed to a faster rate of SOC decomposition in young sites as compared
380 to more prevalent anoxic conditions in older mangrove stands, which may lead to a higher degree of SOC
381 preservation and thus higher SOC stock in older mangrove sediments.

382

383 For all the young sites and Upstream old site, where SOC stocks are lower than the other old sites, the
384 autochthonous contribution of local vegetation to the SOC was estimated to be very low (i.e., 20.7 ± 13 % of
385 the SOC). The allochthonous OC coming from the water column as suspended matter can be considered as
386 the main source of OC found in sediments of these sites. This is supported by the less negative $\delta^{13}\text{C}$ values
387 of the SOC in these areas that ranged between -27.5 and -24.4‰ (Figure 4A-D) and lower C:N ratios of 11.5
388 – 14.9 (Table S2) compared to the other older sites. Generally lower C:N ratios and higher freshwater input



389 of organic matter could indicate faster decomposition, hence resulting in lower SOC contents and stocks
390 (Leopold *et al.*, 2015). Therefore, our data suggest that the majority of the SOC in these sites is not produced
391 from newly fixed CO₂ by the local mangrove vegetation but rather from tidal deposition of material originat-
392 ing from terrestrial, marine or estuarine reservoirs.

393 Furthermore, the old mangrove sites of the Intermediate, Downstream and Marine sites have lower $\delta^{13}\text{C}$
394 values (-28.1 to -26.5‰) and higher C:N ratios (17.7 – 33.9) compared to the young sites and the Upstream
395 old site. In these sites, it is estimated that more than half ($59 \pm 8\%$) of the SOC is of autochthonous origin
396 indicating that a significant portion of locally produced organic matter is preserved in these areas. Other
397 mangrove forests wherein $\delta^{13}\text{C}$ and C:N values of sediments closely match those of the mangrove roots and
398 aboveground vegetation also reported a similar portion of mangrove-derived SOC of 58% (Kristensen *et al.*,
399 2008). This relatively higher contribution of locally produced carbon to the mangrove SOC could explain
400 why these sites have higher SOC contents and stocks than the young mangrove sites, as the OC content in
401 organic material derived from mangrove vegetation is normally higher than that of the suspended sediments
402 (Figure 5A).

403 Finally, it is important to note the comparable SOC stocks and contents of the young and old sites of the
404 Marine zone. This is clearly due to the high SOC content in the upper 0.20 m of the younger sites which
405 compensate for the lower SOC content deeper than 0.20 m, and which results in similar depth-averaged SOC
406 content as in the older sites (Figure 2). Analyses of the cores showed that a high amount of macroscopic
407 vegetation remains were found in the upper 0.20 m of the young Marine site cores.

408

409 **4.2 | SOC variability along the estuarine land-to-sea gradient**

410 We observed SOC contents and stocks to generally increase from zones with low to high salinity (Figure 2
411 and 3). Similar patterns were found in river-influenced estuarine mangrove forests in the Ganges-Brahmapu-
412 tra Delta in the Indian Sundarbans (Donato *et al.*, 2011), the Pichavaram Mangrove in southeast India (Ranjan
413 *et al.*, 2011) and the Mui Ca Mau National Park in the Mekong Delta, Vietnam (Tue *et al.*, 2014). A potential
414 reason could be the higher input of riverine mineral-rich sediments in the more upstream locations of the
415 delta, resulting in higher mineral sediment accretion rates in the lower salinity zones, and diluting the organic
416 matter content in the mangrove sediments. In addition, we found a strong positive correlation (Pearson's $r =$



417 0.96) between the SOC content and C:N ratios (see Figure S3 and S4) of the mangrove sediments. This may
418 suggest that the higher N contents in the more upstream and young sites may contribute to higher mineral-
419 associated carbon and hence, lower SOC contents and stocks.

420

421 From Upstream to Downstream, the sediment $\delta^{13}\text{C}$ values closely match those of the POC from the estu-
422arine waters, while $\delta^{13}\text{C}$ values of the local vegetation biomass differ significantly from the sediment $\delta^{13}\text{C}$
423 values (Figure 4A-D; Figure 5A and B). This suggests that the SOC in the studied mangroves along the land-
424 to-sea gradient mainly consists of allochthonous sources (estimated at $65 \pm 22\%$), while preservation of lo-
425cally produced autochthonous OC into SOC is limited. Fairly similar ranges of $\delta^{13}\text{C}$ (-29.5 to -23.9 ‰) and
426 C:N ($9 - 26.6$) were obtained in the estuarine mangrove of Segara Anakan Lagoon in southern Java, Indonesia
427 (Kusumaningtyas *et al.*, 2019; Jennerjahn 2021), where the majority of the organic matter in the mangrove
428 sediment was also concluded to be externally derived. Additionally, a study of Weiss *et al.* (2016) in the
429 Berau estuary in eastern Kalimantan, Indonesia, also found silt loam sediments (similar to the sediment tex-
430 ture found in the Guayas mangroves, Table S6) mainly composed of externally-derived OC which had a bulk
431 density ($0.4 - 0.7 \text{ g cm}^{-3}$) and $\delta^{13}\text{C}$ values (-29.5 to -25.6 ‰) close to those found in our study (see Table S2).

432 A potential explanation to this observed predominance of externally derived SOC is the tidal range and
433 the quality of the allochthonous and autochthonous organic matter that comes in the Guayas mangrove eco-
434 systems. A study of the contribution of both internal and external inputs of OC in marsh sediments in the
435 Scheldt Estuary, in the Netherlands and Belgium (Van de Broek *et al.*, 2016; Van de Broek *et al.*, 2018),
436 proposed that the burial efficiencies of the different sources of POC are related to their decomposability. For
437 this study area, they suggest that allochthonous POC is composed largely of terrestrial, recalcitrant POC.
438 Consequently, allochthonous POC is expected to decompose relatively slower after burial and remain in
439 sediments for a longer time. In contrast, they argue that the autochthonous POC, derived from local vegeta-
440 tion, is fresh and labile, thus expected to decompose more rapidly than allochthonous recalcitrant POC. Such
441 a difference in the quality of OC sources may potentially explain why there is a lower contribution of autoch-
442 thonous OC in mangrove sediments of our study sites. As the Guayas system has a high tidal range of 3-5 m,
443 this specific environmental condition may allow better drainage of the mangrove sediments during low tides,



444 enabling deeper aeration of sediment profiles, and hence resulting in higher decomposition rates and less
445 preservation of more labile OC from the local vegetation.

446

447 **4.3 | Downcore variations of organic matter composition**

448 In general, the individual SOC content, $\delta^{13}\text{C}$ and C:N depth profiles (Figures 2 and 4 and Figure S2 and S3)
449 of each site are relatively uniform. This can be potentially explained by the bioturbation effect of red crabs
450 (*Ucides occidentalis*) that were abundantly present in the mangrove sampling areas (visible as burrowing
451 holes and small mounds of burrowed material on top of the sediment surface). The active digging and mainte-
452 nance of burrows by crabs, to escape from predation and from extreme environmental settings (Kristensen,
453 2007), may be expected to mix the upper column of the mangrove sediments, making the profile almost
454 vertically homogenous.

455 The old mangrove sites in the Intermediate, Downstream and Marine zones showed a limited but gradual
456 increase in SOC content (Figure 2B-D) from the top layer down to 60 cm, which is accompanied by downcore
457 increases in OC density (Figure S2). According to Kusumaningtyas *et al.* (2019), such pattern may be an
458 indication of predominance of autochthonous mangrove organic matter in sediments originating from below-
459 ground OC input (i.e. root material). The fact that we find such pattern in old sites, and not in young ones,
460 could further support the finding of higher contribution of autochthonous sources to SOC in our old mangrove
461 sites.

462

463 **4.4 | Implications for management of mangrove forests as carbon sinks**

464 This study estimates that large fractions of the mangrove SOC come from allochthonous sources, which are
465 originating from CO_2 that has been sequestered in other ecosystems (terrestrial, estuarine and/or marine) and
466 transported and deposited in the mangroves. Additionally, these could also be old-aged carbon, already se-
467 questered for a significant amount of time (Van de Broek *et al.*, 2018). This would imply that contemporary
468 carbon capture by the mangrove ecosystem itself, contributes only partly and relatively little to long-term
469 SOC storage. This finding is particularly relevant for budgeting the potential of mangrove ecosystems to



470 mitigate climate change under nature-based mitigation programs such as PES and REDD+ (Yee, 2010; Loca-
471 telli *et al.*, 2014; Nam *et al.*, 2015). As a consequence, relying on estimates of total SOC stocks in mangroves,
472 may seriously overestimate the contribution of mangroves to contemporary CO₂ sequestration by the man-
473 grove ecosystem itself.

474 We found that older mangroves store larger amounts of SOC than younger mangroves. This may suggest
475 the importance of conservation of especially old-grown mangroves and, while measures to promote the for-
476 mation of new young mangroves are still useful, it may provide less carbon storage on short-term as compared
477 to old mangroves. How long it takes before young mangroves reach SOC contents and stocks similar to old
478 mangroves remains unknown. However, it is important to mention that sediment accretion rates may be
479 higher on young than old mangroves, for reasons discussed above (see 4.1), which could partly compensate
480 for the lower SOC contents of young mangroves, and therefore SOC accumulation rates may be more similar
481 between young and old mangroves.

482 Our results also show that SOC contents and stocks in old mangroves increase from river- to marine-
483 dominated sites. This suggests that conservation and expansion of mangroves in the marine-dominated part
484 of estuaries may be most effective for carbon storage policies. However, sediment accretion rates may be
485 higher in river-dominated sites which could lead to similar SOC accumulation rates with marine-dominated
486 sites. Hence further research on linking sediment accretion and SOC accumulation rates are imperative to
487 shed light to these uncertainties.

488

489 **5 | CONCLUSIONS**

490 Our findings show strong indications that the age of the mangrove stand as well as its position along the land-
491 to-sea gradient play a vital role in the amount and sources of carbon stored in the mangrove sediments in the
492 Guayas delta (Ecuador). Young mangroves are found to have lower SOC contents and stocks than old man-
493 groves. This may be potentially due to higher mineral-rich sediment inputs on initially lower elevated,
494 younger mangroves, which dilutes the SOC content in the mangrove sediments. A pattern of increasing SOC
495 stocks (and corresponding SOC content) from river- to marine-dominated sites was also found, which may
496 be attributed to a similar dilution effect, where higher riverine mineral-rich sediment inputs lead to lower



497 SOC contents on more river-dominated, lower salinity sites. Based on $\delta^{13}\text{C}$ values and elemental C:N ratios,
498 we identified that the SOC of the young mangrove sites is predominantly of allochthonous composition (79
499 $\pm 13\%$) whereas the old sites had only a slight dominance of autochthonous SOC ($59 \pm 8\%$). Finally, our
500 study highlights that only a portion of the SOC stored in mangrove ecosystems is originating from con-
501 temporary CO_2 sequestration by the ecosystem itself, which is particularly relevant to consider when
502 designing and valuing nature-based climate mitigation programs based on mangrove reforestation.

503

504 **Funding Information**

505 Fonds Wetenschappelijk Onderzoek – Vlaanderen (FWO, Research Foundation Flanders, PhD grant no.
506 FWO R.H.S., 1168520N and FWO project grant no. G060018N), Vlaamse Interuniversitaire Raad -
507 Universitaire Ontwikkelingssamenwerking (VLIR-UOS), ActUA Prijs – University of Antwerp

508

509 **REFERENCES**

510 Abril, G., Nogueira, M., Etcheber, H., Cabeçadas, G., Lemaire, E., & Brogueira, M. J. (2002). Behaviour of
511 organic carbon in nine contrasting European estuaries. *Estuarine, coastal and shelf science*, 54(2), 241-262.

512 Adame, M. F., Santini, N. S., Tovilla, C., Vázquez-Lule, A., Castro, L., & Guevara, M. (2015). Carbon stocks
513 and soil sequestration rates of tropical riverine wetlands. *Biogeosciences*, 12(12), 3805-3818.

514 Allen, J. R. L. (1990). Salt-marsh growth and stratification: a numerical model with special reference to the
515 Severn Estuary, southwest Britain. *Marine Geology*, 95(2), 77-96.

516 Alongi, D. M. (2012). Carbon sequestration in mangrove forests. *Carbon management*, 3(3), 313-322.

517 Alongi, D. M. (2014). Carbon cycling and storage in mangrove forests. *Annual review of marine science*, 6,
518 195-219.

519 Arreaga Vargas, P. (2000). Análisis del comportamiento de la salinidad (intrusión salina) en el sistema Río
520 Guayas Canal de Jambelí como parte del cambio climático.

521 Atwood, T. B., Connolly, R. M., Almahasheer, H., Carnell, P. E., Duarte, C. M., Lewis, C. J. E., ... & Serrano,
522 O. (2017). Global patterns in mangrove soil carbon stocks and losses. *Nature Climate Change*, 7(7), 523.



- 523 Barr, J. G., Engel, V., Fuentes, J. D., Zieman, J. C., O'Halloran, T. L., Smith, T. J., & Anderson, G. H. (2010).
524 Controls on mangrove forest-atmosphere carbon dioxide exchanges in western Everglades National Park.
525 *Journal of Geophysical Research: Biogeosciences*, 115(G2).
- 526 Borges, A.V., Abril, G. (2011) Carbon Dioxide and Methane Dynamics in Estuaries. In: Wolanski E,
527 McLusky DS (eds) *Treatise on Estuarine and Coastal Science*, vol 5. Academic Press, Waltham, 119–161.
- 528 Bouillon, S., Dahdouh-Guebas, F., Rao, A. V. V. S., Koedam, N., & Dehairs, F. (2003). Sources of organic
529 carbon in mangrove sediments: variability and possible ecological implications. *Hydrobiologia*, 495(1-3),
530 33-39.
- 531 Bouillon, S., Borges, A. V., Castañeda-Moya, E., Diele, K., Dittmar, T., Duke, N. C., ... & Rivera-Monroy,
532 V. H. (2008). Mangrove production and carbon sinks: a revision of global budget estimates. *Global Biogeo-*
533 *chemical Cycles*, 22(2).
- 534 Burkett, V., & Kusler, J. (2000). Climate change: potential impacts and interactions in wetlands of the united
535 states 1. *JAWRA Journal of the American Water Resources Association*, 36(2), 313-320.
- 536 Cifuentes, L. A., Coffin, R. B., Solorzano, L., Cardenas, W., Espinoza, J., & Twilley, R. R. (1996). Isotopic
537 and elemental variations of carbon and nitrogen in a mangrove estuary. *Estuarine, Coastal and Shelf Science*,
538 43(6), 781-800.
- 539 Craft, C. (2007). Freshwater input structures soil properties, vertical accretion, and nutrient accumulation of
540 Georgia and US tidal marshes. *Limnology and oceanography*, 52(3), 1220-1230.
- 541 Cruz-Orozco, R. (1974). Morphodynamics and sedimentation of the Rio Guayas delta, Ecuador.
- 542 Cucalón, E. (1989). Oceanographic characteristics off the coast of Ecuador. A sustainable shrimp mariculture
543 industry for Ecuador, pp. University of Rhode Island, Narragansett, RI: Coastal Resources Center.
- 544 Donato, D. C., Kauffman, J. B., Murdiyarsa, D., Kurnianto, S., Stidham, M., & Kanninen, M. (2011). Man-
545 groves among the most carbon-rich forests in the tropics. *Nature geoscience*, 4(5), 293.
- 546 Duarte, C. M., Middelburg, J. J., & Caraco, N. (2004). Major role of marine vegetation on the oceanic carbon
547 cycle. *Biogeosciences discussions*, 1(1), 659-679.



- 548 Duke, N.C., Meynecke, J.O., Dittmann, S., Ellison, A.M., Anger, K. et al. (2007). A world without man-
549 groves. *Science* 317: 41.
- 550 French, J. R. (1993). Numerical simulation of vertical marsh growth and adjustment to accelerated sea-level
551 rise, north Norfolk, UK. *Earth Surface Processes and Landforms*, 18(1), 63-81.
- 552 Hansen, K., Butzeck, C., Eschenbach, A., Gröngröft, A., Jensen, K., & Pfeiffer, E. M. (2017). Factors influ-
553 encing the organic carbon pools in tidal marsh soils of the Elbe estuary (Germany). *Journal of soils and*
554 *sediments*, 17(1), 47-60.
- 555 Jacotot, A., Marchand, C., & Allenbach, M. (2018). Tidal variability of CO₂ and CH₄ emissions from the
556 water column within a *Rhizophora* mangrove forest (New Caledonia). *Science of the Total Environment*,
557 631, 334-340.
- 558 Jennerjahn, T. C. (2020). Relevance and magnitude of 'Blue Carbon' storage in mangrove sediments: Carbon
559 accumulation rates vs. stocks, sources vs. sinks. *Estuarine, Coastal and Shelf Science*, 247, 107027.
- 560 Jennerjahn, T. C. (2021). Relevance of allochthonous input from an agriculture-dominated hinterland for
561 "Blue Carbon" storage in mangrove sediments in Java, Indonesia. In *Dynamic Sedimentary Environments*
562 *of Mangrove Coasts* (pp. 393-414). Elsevier.
- 563 Kirwan, M. L., Temmerman, S., Skeeahan, E. E., Guntenspergen, G. R., and Fagherazzi, S. (2016). Overesti-
564 mation of marsh vulnerability to sea level rise: *Nature Climate Change*, v. 6, p. 253-260.
- 565 Kristensen, E. (2007). Mangrove crabs as ecosystem engineers; with emphasis on sediment processes. *Jour-
566 nal of sea Research*, 59(1-2), 30-43.
- 567 Kristensen, E., Bouillon, S., Dittmar, T., & Marchand, C. (2008). Organic carbon dynamics in mangrove
568 ecosystems: a review. *Aquatic botany*, 89(2), 201-219.
- 569 Kusumaningtyas, M. A., Hutahaean, A. A., Fischer, H. W., Pérez-Mayo, M., Ransby, D., & Jennerjahn, T.
570 C. (2019). Variability in the organic carbon stocks, sources, and accumulation rates of Indonesian mangrove
571 ecosystems. *Estuarine, Coastal and Shelf Science*, 218, 310-323.
- 572 Leopold, A., Marchand, C., Deborde, J., & Allenbach, M. (2015). Temporal variability of CO₂ fluxes at the
573 sediment-air interface in mangroves (New Caledonia). *Science of the Total Environment*, 502, 617-626.



- 574 Locatelli, T., Binet, T., Kairo, J. G., King, L., Madden, S., Patenaude, G., ... & Huxham, M. (2014). Turning
575 the tide: how blue carbon and payments for ecosystem services (PES) might help save mangrove forests.
576 *Ambio*, 43(8), 981-995.
- 577 Lovelock, C. E., Sorrell, B. K., Hancock, N., Hua, Q., & Swales, A. (2010). Mangrove forest and soil devel-
578 opment on a rapidly accreting shore in New Zealand. *Ecosystems*, 13(3), 437-451.
- 579 Maher, D. T., Santos, I. R., Golsby-Smith, L., Gleeson, J., & Eyre, B. D. (2013). Groundwater-derived dis-
580 solved inorganic and organic carbon exports from a mangrove tidal creek: The missing mangrove carbon
581 sink?. *Limnology and Oceanography*, 58(2), 475-488.
- 582 Marchand, C., Baltzer, F., Lallier-Vergès, E., & Albéric, P. (2004). Pore-water chemistry in mangrove sedi-
583 ments: relationship with species composition and developmental stages (French Guiana). *Marine Geology*,
584 208(2-4), 361-381.
- 585 Marchand, C., Lallier-Vergès, E., Baltzer, F., Albéric, P., Cossa, D., & Baillif, P. (2006). Heavy metals dis-
586 tribution in mangrove sediments along the mobile coastline of French Guiana. *Marine chemistry*, 98(1), 1-
587 17.
- 588 Marchand, C. (2017). Soil carbon stocks and burial rates along a mangrove forest chronosequence (French
589 Guiana). *Forest ecology and management*, 384, 92-99.
- 590 Mcleod, E., Chmura, G. L., Bouillon, S., Salm, R., Björk, M., Duarte, C. M., ... & Silliman, B. R. (2011). A
591 blueprint for blue carbon: toward an improved understanding of the role of vegetated coastal habitats in
592 sequestering CO₂. *Frontiers in Ecology and the Environment*, 9(10), 552-560.
- 593 Mueller, P., Ladiges, N., Jack, A., Schmiedl, G., Kutzbach, L., Jensen, K., and Nolte, S. (2019). Assessing
594 the long-term carbon-sequestration potential of the semi-natural salt marshes in the European Wadden Sea:
595 *Eco-sphere*, v. 10, no. 1.
- 596 Murdiyarso, D., Purbopuspito, J., Kauffman, J. B., Warren, M. W., Sasmito, S. D., Donato, D. C., ... &
597 Kurnianto, S. (2015). The potential of Indonesian mangrove forests for global climate change mitigation.
598 *Nature Climate Change*, 5(12), 1089.
- 599 Nam, M. V. (2015). *Mangroves for the Future Phase III–National Strategic Action Plan (2015–2018)*.



- 600 Pendleton, L., Donato, D. C., Murray, B. C., Crooks, S., Jenkins, W. A., Sifleet, S., ... & Megonigal, P.
601 (2012). Estimating global “blue carbon” emissions from conversion and degradation of vegetated coastal
602 ecosystems. *PloS one*, 7(9), e43542.
- 603 Pethick, J. S. (1981). Long-term accretion rates on tidal salt marshes. *Journal of Sedimentary Research*, 51(2),
604 571-577.
- 605 Polidoro BA, Carpenter KE, Collins L, Duke NC, Ellison AM, et al. (2010) The Loss of Species: Mangrove
606 Extinction Risk and Geographic Areas of Global Concern. *PLoS ONE* 5(4): e10095. doi:10.1371/jour-
607 nal.pone.0010095
- 608 R Core Team (2017). A language and environment for statistical computing. R Foundation for Statistical
609 Computing, Vienna, Austria 2014. URL:(<https://www.R-project.org>).
- 610 Ranjan, R. K., Routh, J., Ramanathan, A. L., & Klump, J. V. (2011). Elemental and stable isotope records of
611 organic matter input and its fate in the Pichavaram mangrove–estuarine sediments (Tamil Nadu, India). *Ma-
612 rine Chemistry*, 126(1-4), 163-172.
- 613 Reynaud, J. Y., Witt, C., Pazmiño, A., & Gilces, S. (2018). Tide-dominated deltas in active margin basins:
614 Insights from the Guayas estuary, Gulf of Guayaquil, Ecuador. *Marine Geology*, 403, 165-178.
- 615 Saintilan, N., Rogers, K., Mazumder, D., & Woodroffe, C. (2013). Allochthonous and autochthonous contri-
616 butions to carbon accumulation and carbon store in southeastern Australian coastal wetlands. *Estuarine,
617 Coastal and Shelf Science*, 128, 84-92.
- 618 Schile, L. M., Kauffman, J. B., Crooks, S., Fourqurean, J. W., Glavan, J., & Megonigal, J. P. (2017). Limits
619 on carbon sequestration in arid blue carbon ecosystems. *Ecological Applications*, 27(3), 859-874.
- 620 Siikamäki, J., Sanchirico, J. N., & Jardine, S. L. (2012). Global economic potential for reducing carbon di-
621 oxide emissions from mangrove loss. *Proceedings of the National Academy of Sciences*, 109(36), 14369-
622 14374.
- 623 Sturm, K., Werner, U., Grinham, A., & Yuan, Z. (2017). Tidal variability in methane and nitrous oxide emis-
624 sions along a subtropical estuarine gradient. *Estuarine, Coastal and Shelf Science*, 192, 159-169.



- 625 Taillardat, P., Friess, D. A., & Lupascu, M. (2018). Mangrove blue carbon strategies for climate change
626 mitigation are most effective at the national scale. *Biology Letters*, 14(10), 20180251.
- 627 Temmerman, S., Govers, G., Meire, P., & Wartel, S. (2003). Modelling long-term tidal marsh growth under
628 changing tidal conditions and suspended sediment concentrations, Scheldt estuary, Belgium. *Marine Geol-*
629 *ogy*, 193(1-2), 151-169.
- 630 Temmerman, S., Govers, G., Wartel, S., and Meire, P. (2004). Modelling estuarine variations in tidal marsh
631 sedimentation: response to changing sea level and suspended sediment concentrations: *Marine Geology*, v.
632 212, p. 1-19.
- 633 Tue, N.T., Quy, T.D., Hamaoka, H., Nhuan, M.T., and Omori, K. (2012) Sources and Exchange of Particulate
634 Organic Matter in an Estuarine Mangrove Ecosystem of Xuan Thuy National. 1060–1068.
- 635 Tue, N. T., Dung, L. V., Nhuan, M. T., & Omori, K. (2014). Carbon storage of a tropical mangrove forest in
636 Mui Ca Mau National Park, Vietnam. *Catena*, 121, 119-126.
- 637 Twilley, R. R., Chen, R. H., & Hargis, T. (1992). Carbon sinks in mangroves and their implications to carbon
638 budget of tropical coastal ecosystems. *Water, Air, and Soil Pollution*, 64(1-2), 265-288.
- 639 Twilley, R. R., Gottfried, R. R., Rivera-Monroy, V. H., Zhang, W., Armijos, M. M., & Boderó, A. (1998).
640 An approach and preliminary model of integrating ecological and economic constraints of environmental
641 quality in the Guayas River estuary, Ecuador. *Environmental Science & Policy*, 1(4), 271-288.
- 642 Twilley, R. R., Cárdenas, W., Rivera-Monroy, V. H., Espinoza, J., Suescum, R., Armijos, M. M., & Solór-
643 zano, L. (2001). The Gulf of Guayaquil and the Guayas river estuary, Ecuador. In *Coastal marine ecosystems*
644 *of Latin America* (pp. 245-263). Springer, Berlin, Heidelberg.
- 645 Van de Broek, M., Temmerman, S., Merckx, R., & Govers, G. (2016). Controls on soil organic carbon stocks
646 in tidal marshes along an estuarine salinity gradient. *Biogeosciences*, 13(24), 6611-6624.
- 647 Van de Broek, M., Vandendriessche, C., Poppelmonde, D., Merckx, R., Temmerman, S., and Govers, G.
648 (2018). Long-term organic carbon sequestration in tidal marsh sediments is dominated by old-aged alloch-
649 thonous inputs in a macrotidal estuary: *Global Change Biology*, v. 24, no. 6, p. 2498-2512.



650 Weiss, C., Weiss, J., Boy, J., Iskandar, I., Mikutta, R., & Guggenberger, G. (2016). Soil organic carbon stocks
651 in estuarine and marine mangrove ecosystems are driven by nutrient colimitation of P and N. *Ecology and*
652 *evolution*, 6(14), 5043-5056.

653 Więski, K., Guo, H., Craft, C. B., & Pennings, S. C. (2010). Ecosystem functions of tidal fresh, brackish, and
654 salt marshes on the Georgia coast. *Estuaries and Coasts*, 33(1), 161-169.

655 Yee, S. (2010). REDD and BLUE carbon: carbon payments for mangrove conservation.

656

657

658

659

660

661

662

663

664

665

666

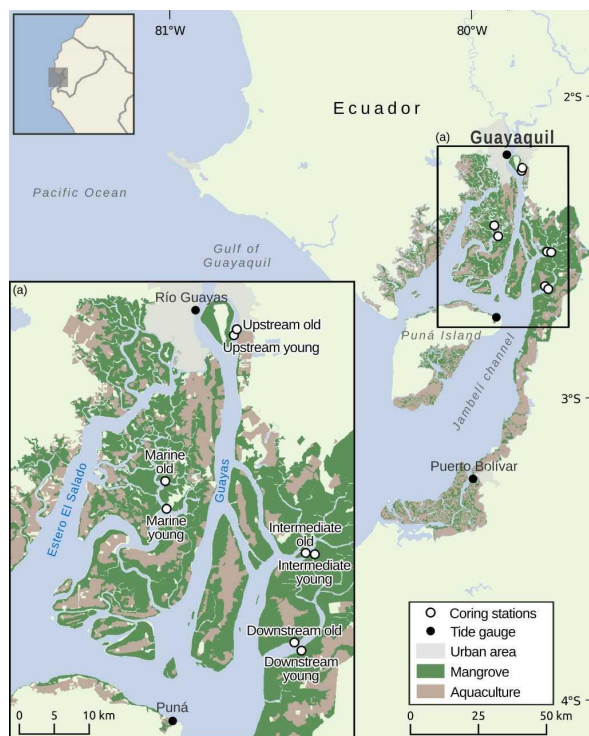
667

668

669



670



671

672 **Figure 1** Map of the Guayas Delta showing the locations of the sampled young and old mangrove systems along
673 an estuarine land-to-sea gradient.

674

675

676

677

678

679

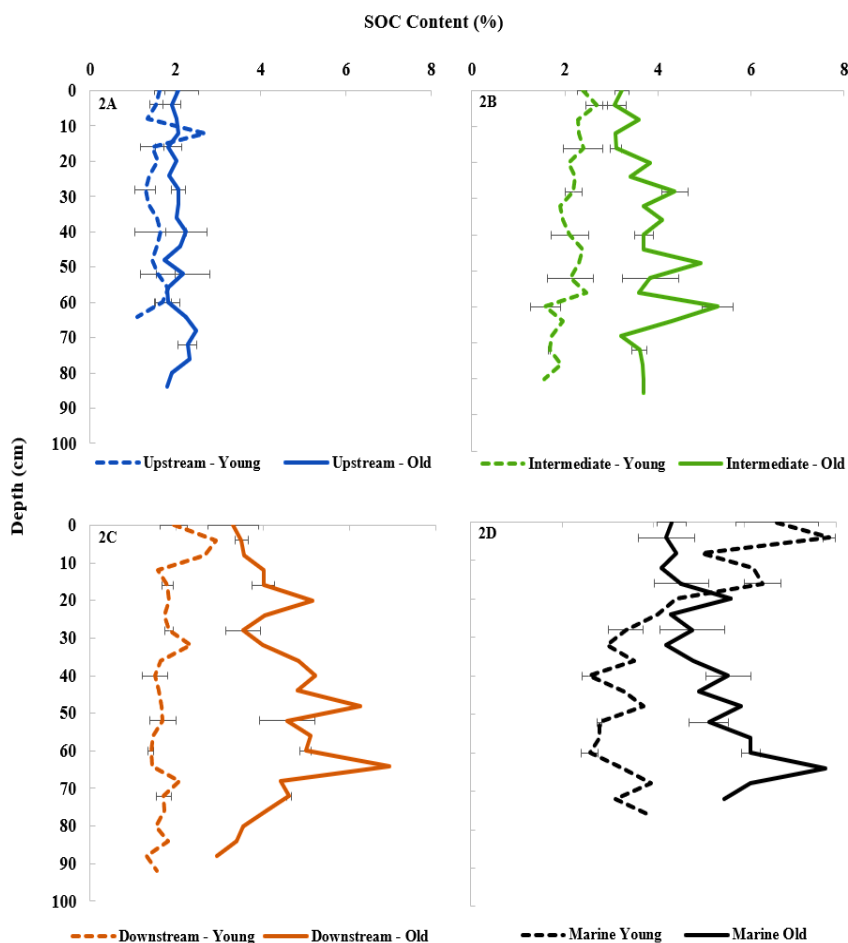
680

681

682



683



684

685 **Figure 2** Depth profiles of SOC content (%) for all sites. Fig.2A: Upstream Zone; Fig.2B: Intermediate
686 Zone; Fig.2C: Downstream Zone; Fig.2D: Marine Zone. Data points show the average OC% of sediment
687 samples from three replicate cores per site and error bars for specific points represent the standard deviation.

688

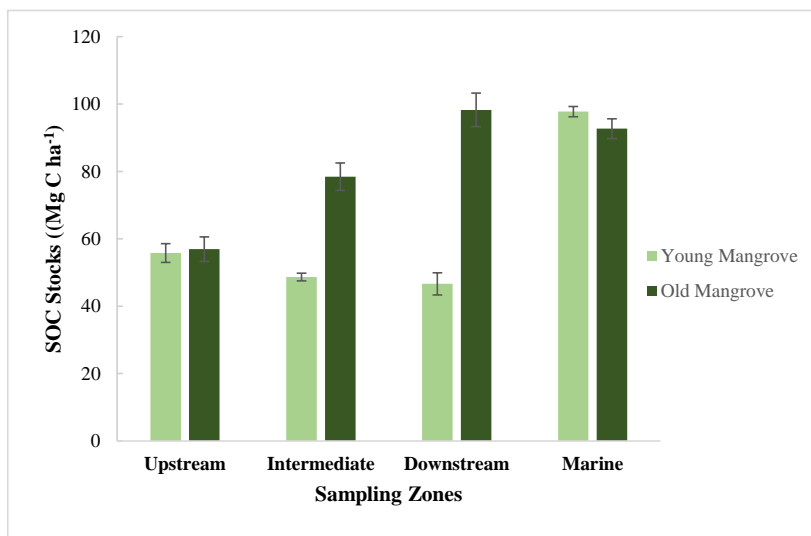
689

690

691



692



701

702 **Figure 3** Total sediment organic carbon (SOC) stocks (Mg C ha⁻¹) for the upper 0.64 m of the vertical
703 sampling profiles. Standard deviation was calculated based on the SOC stocks of three replicate cores per
704 site.

705

706

707

708

709

710

711

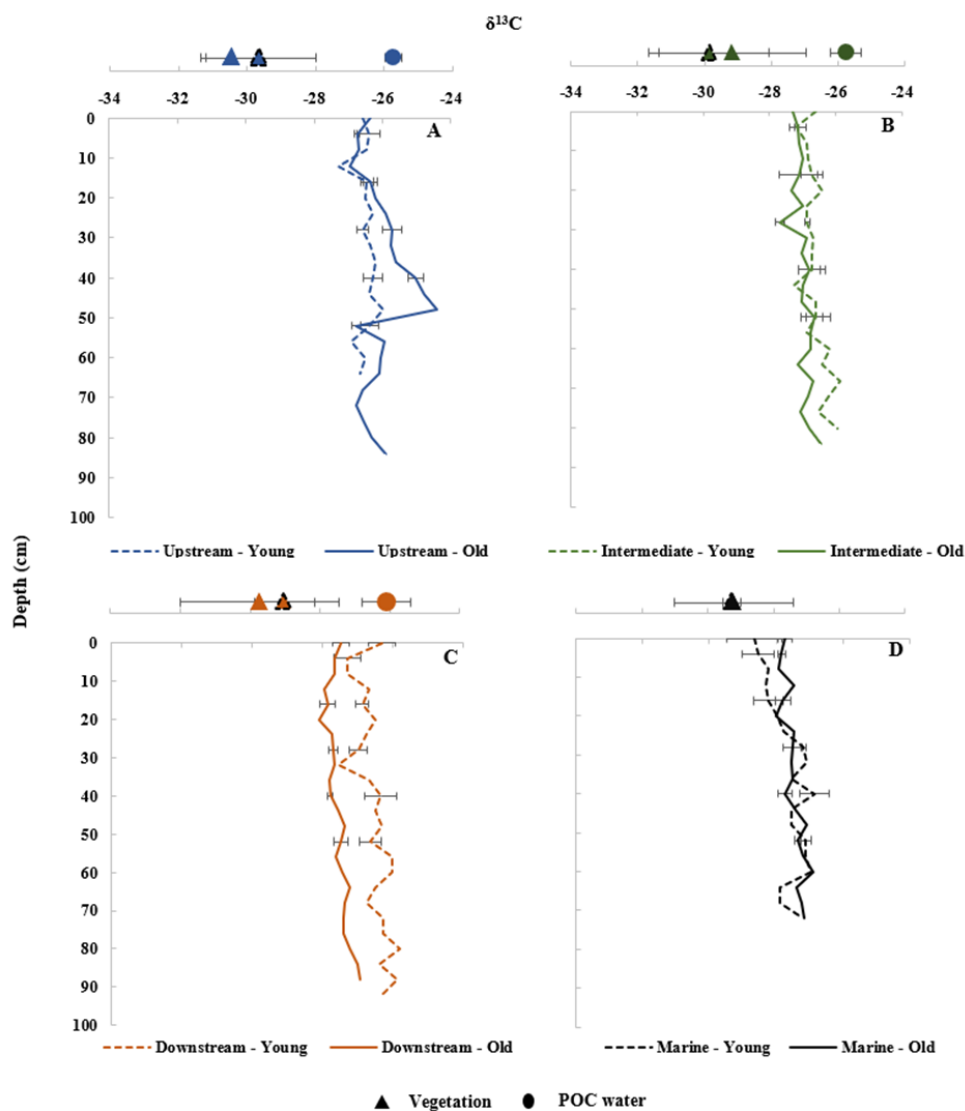
712

713



714

715



716

717 **Figure 4** Depth profiles of $\delta^{13}\text{C}$ of sediment cores and $\delta^{13}\text{C}$ of autochthonous above and belowground veg-
718 etation (triangles) and allochthonous POC (circles) of adjacent water bodies for the sites (values are provided
719 in Table S2, S4 and S5). Fig.4A: Upstream Zone; Fig.4B: Intermediate Zone; Fig.4C: Downstream Zone;
720 Fig.4D: Marine Zone. Average POC data in dry and wet seasons (both high and low tides) were used. POC



721 data are considered representative for the water flooding both the adjacent young and old sites in each zone.
722 Vegetation data represent average values for roots, sun-shaded and sun-exposed green leaves, senescent
723 leaves, leaf litter, live twigs, and branches, per young and old site in each zone. No data on POC and vegeta-
724 tion were obtained for the Marine site. Error bars represent the standard deviation of sediment subsamples
725 taken at 0.04m depth increment for the three replicate cores and 8 types of vegetation samples (see Section
726 2.2.) taken per site and 8 POC samples taken per sampling zone.

727

728

729

730

731

732

733

734

735

736

737

738

739

740

741

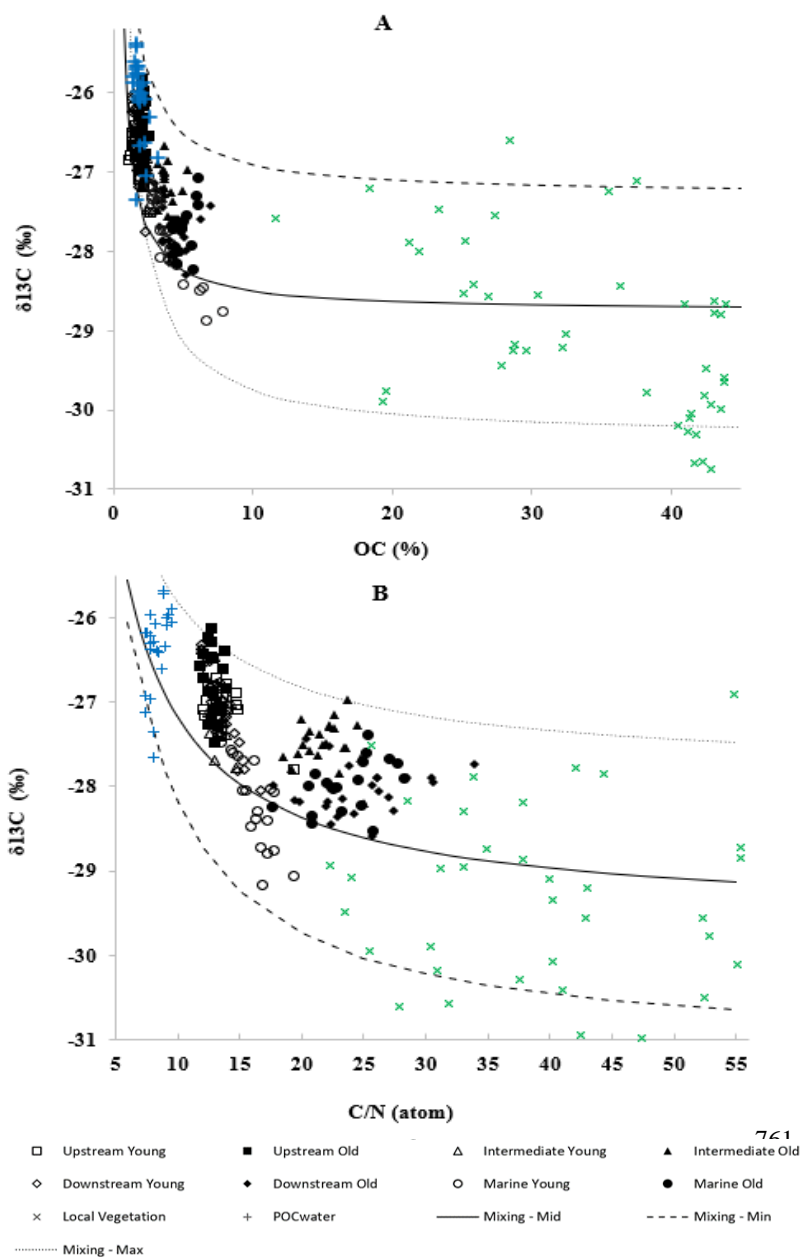
742

743



744

745



763

761



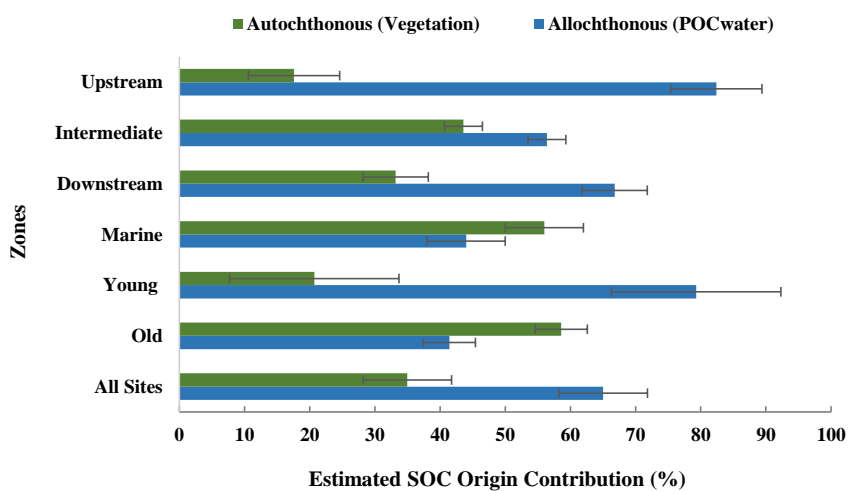
764 **Figure 5 (A)** Stable carbon isotope ratios $\delta^{13}\text{C}$ (‰) versus SOC content (%) and **(B)** $\delta^{13}\text{C}$ (‰) values versus
765 C/N (atom) ratios of all sampled sites. Different curves correspond to different end-member values for the
766 sources (see text for details).

767

768

769

770



781

782 **Figure 6** Estimated contribution (%) of allochthonous and autochthonous origins to the SOC of the study
783 sites. Averages and standard deviations were calculated from three replicate cores per site.

784